A Universal, Fully Automated High Throughput Screening Assay for Pyrophosphate and Phosphate Release from Enzymatic Reactions

Scott D. Pegan*, Yang Tian, Valerie Sershon and Andrew D. Mesecar*

Center for Pharmaceutical Biotechnology and the Department of Medicinal Chemistry and Pharmacognosy, the University of Illinois at Chicago, Chicago, IL 60607, USA

Abstract: The malachite green assay is often used for measuring the presence of inorganic mono-phosphate concentrations. Some studies have adapted this assay for use in monitoring enzymatic reactions and have suggested its potential use in high throughput screening (HTS). With the increasing availability of laboratory automation, some studies are starting to explore the possibility of conducting limited, semi-automated versions of the assay. Here we report the optimization and complete adaptation of the malachite green assay to a fully automated, HTS platform that can be performed unattended with standard, commercially available, automated liquid-handling systems. The assay is universal for the majority of enzymes that release phosphate or pyrophosphate. Moreover, the assay is fully scalable from smaller drug screening efforts (~20,000 wells per day) to ultra-high throughput environments (~200,000 wells per day). The assay uses cost-effective, commercially available reagents, and can be used to perform automated IC_{50} value and kinetic parameter determination. Finally, we demonstrate the utility of the assay *via* the initial, primary screening of 100,080 compounds against two target enzymes from *Bacillus anthracis*, O-succinylbenzoyl-CoA synthetase and nicotinate mononucleotide adenylyltransferase.

Keywords: Malachite green, high throughput screening, pyrophosphatase, assay techniques, phosphate.

INTRODUCTION

Enzymes that release phosphate in the form of pyrophosphate or monophosphate (ERPs) comprise one of the most diverse sets of proteins with respect to the reactions that they catalyze. ERP members exist as simple pyrophosphatases, protein phosphatases, ATPases and GTPases as well as adenyltransferase and synthetases. Not surprisingly, many of these enzymes have been shown to mediate essential pathways for sustaining bacterial life in *Bacillus subtillus* making them attractive targets for drug development [1]. To capitalize on the prevalence of these enzymes in several critical cellular pathways, a HTS assay that requires minimal adaptation between ERPs, yet allows for large-scale HTS with standard laboratory resources, is required. To probe the potential for developing such a universal assay for screening ERPs against large compound libraries, we employed two diverse pharmaceutical targets from *Bacillus anthracis*, O-succinylbenzoyl-CoA synthetase (OSB-CoA synthetase; EC 6.2.1.26) and nicotinate mononucleotide adenyltransferase (NMAT; EC 2.7.7.1). OSB-CoA synthetase and NMAT each catalyze critical reactions essential to the growth and survival of *B. anthracis* and other bacteria. Although these two reactions generate entirely different products, both enzymes can be regarded as nucleotidases (Fig. **1A**).

OSB-CoA synthetase catalyzes the fourth reaction in the *B. anthracis* menaquinone biosynthetic pathway, which is responsible for generating the key electron transport molecule menaquinone (MK-8) [2, 3]. To form OSB-CoA, OSB-CoA synthetase first transfers the AMP protion of ATP to O-succinylbenzoate (OSB) to form an OSB-AMP intermediate and the first product of the reaction, pyrophosphate (PP_i; Fig. **1B**). During the second step, CoA reacts with OSB-AMP to form OSB-CoA and AMP [2]. The kinetic mechanism for the OSB-synthetase reaction is an ordered Bi Uni Uni Bi Iso ping-pong reaction with ATP binding first followed by the binding of OSB. The release of product occurs in the order of PP_i followed by OSB-CoA and then AMP [4].

Whereas OSB-CoA synthetase is critical for the electron transport chain, NMAT serves as a key enzyme in the bacterial synthesis of NAD(P) [1, 5]. NMAT's role in the pathway is the generation of nicotinate adenine dinucleotide (NaAD) and PP_i from nicotinate mono-nucleotide (NaMN) and ATP (Fig. **1C**). NMAT utilizes a random bi bi kinetic mechanism with negative cooperatively associated with the binding of substrates [6]. Recent reports have identified NMAT and other enzymes in the pathway as undergoing significant up-regulation during the critical growth phase of *Bacillus anthracis* in macrophages, suggesting NMAT as a potential drug target [5].

Currently, there are several assays for both enzymes that could be potentially adapted to HTS (Table **1**). Some of these assays are enzyme specific, while others exploit the production of PP_i. OSB-CoA synthetase specific assays include the detection of the product AMP or the detection of DHNA-CoA formation that is generated *via* coupling of the OSB-CoA reaction to the downstream reaction of DHNA-CoA synthetase [4, 7, 8]. Options for NMAT specific assays are more limited since AMP becomes fused to NaMN through the reaction. However, a low-throughput method of detecting NaAD formation *via* HPLC has been used to measure the activity of NMAT [6, 9].

*Address correspondence to these authors at the Center for Pharmaceutical Biotechnology, University of Illinois at Chicago, 900 South Ashland Avenue (M/C 870), Chicago, IL 60607-7173, USA; Tel. 312-996-1877; Fax: 312-413-9303; E-mails: mesecar@uic.edu or pegan@uic.edu

1386-2073/10 $55.00+.00

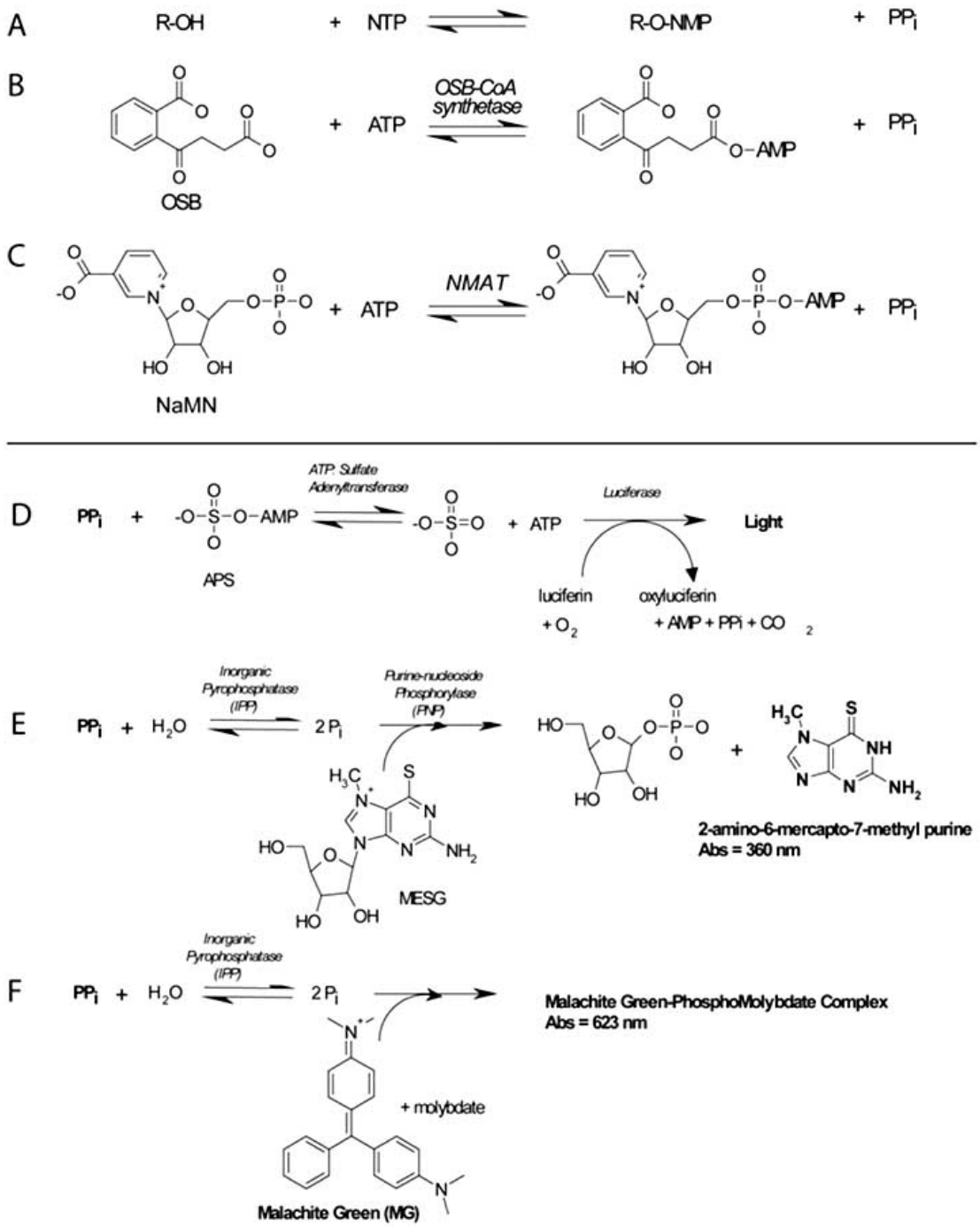

Fig. (1). ERPs that catalyze adenyltransferase reactions. (**A**) General adenyltransferase reaction. (**B**) OSB-CoA synthetase catalyzed reaction (**C**) NMAT catalyzed reaction. Preferred inorganic phosphatae (P_i)-based detection assays. (**D**) Adenyltransferase-Luciferase based assay. (**E**) 2-amino-6-mercapto-7-methyl purine (MESG)-based assay. (**F**) Malachite Green assay.

There are currently four predominant assays for measuring PP_i production that are used routinely (Fig. **1D-F**). The first is a luminescence assay that uses ATP sulfate adenyltransferase to produce ATP from adenine 5'-phosphosulfate and PPi. The ATP produced is directly coupled to the luciferase reaction where it reacts with luciferin to produce light (Fig. **1D**). Although this assay has been used to great success in DNA sequencing and utilized in a few other applications for pyrophosphate detection, the assay requires that ATP be produced continually and in low concentrations for detection. In contrast, ERPs such as OSB-synthetase and NMAT require that high concentrations of ATP be present in their assays which would thereby interfere with detection [10, 11].

A fluorescence-based method for detection of PP_i also recently became available. This assay relies on monophosphate binding to a modified, coumarin labeled, phosphate-binding protein purified from *Escherichia coli* (PBP) [12]. With a K_d of 0.1 μM for Pi, the PBP assay is a sensitive assay; however, the required *N*-[2-(1-

Table 1. Current Assays Available for NMAT and OSB-CoA Synthetase

Assay Type	Enzyme Specific	Fully Commercially Available	Sensitivity	Reagent Cost (Each Well)	Complexity	Reporting Abs Range (nm)	Assay Type
Malachite Green	No	Yes	1-30 μM P_i	<5 cents	low, one coupled enzyme	623	End-point
MESG	No	Yes	>1μM P_i	>10 cents	medium, two coupled enzyme	380	Continuous
MenB coupled	Yes	No	>10 μM OSB-CoA	<5 cents	low, one coupled enzyme	392	Continuous
MDCC-PBP	No	No	>0.1 μM P_i	>15 cents	medium, two coupled enzyme	ex 430 / em 450	Continuous
NMAT HPLC Assay	Yes	Yes	>2 μM NaaD	>10 cents	low, no couple enzyme required	NA	End-point
AMP detection	No*	Yes	> 2 μM P_i	>16 cents	high, three coupled enzyme	340	Continuous

*Assay can only be performed on reactions that produce AMP.

maleimidyl)ethyl]-7-(diethylamino)coumarin-3-carboxamide (MDCC)-labeled PBP is not commercially available and requires synthesis *via* a complex, multi-step process involving protein purification of a mutated version of PBP, modification with MDCC, and removal of indigenous monophosphate using purine nucleoside phosphorylase and 7-methylguanosine (MEG) [12]. As a result, this assay is unlikely to be adapted to HTS due to its complexity and associated expense (Table **1**).

The remaining two assays for detection of PP_i are colorimetric. The amino-6-mercapto-7-methylpurine ribonucleoside (MESG) assay relies on the detection of a 2-amino-6-mercapto-7-methylpurine product formed from the reaction of MESG and free mono-inorganic phosphate (P_i) by purine-nucleoside phosphorylase (PNP) [13]. In comparison to the MESG assay, the malachite green assay (MG) capitalizes on the strong absorption shifts created by P_i entering into a malachite green, phosphomolydbate complex at low pH [14].

Although all the aforementioned assay methods are valid and have the sensitivity required for inhibitor identification, we weighed the cost, commercial availability, complexity, and wavelength range for our final selection criteria. In addition, we sought an assay that could be used universally for any enzyme that releases PP_i or P_i. For each of these criteria, the malachite green assay for P_i detection showed the most potential. Unlike most of the other assays, MG can be adapted for ERPs that release pyrophosphatase by requiring only one coupling enzyme to be added, inorganic pyrophosphatase (IPP), to cleave PP_i to monophosphate P_i (Fig. **1E**, **F**). This minimizes the number of enzymes that would have to be counter-screened to differentiate any false positive hits from potential inhibitors identified during screening. Furthermore, the assay requires no rare or commercially unavailable substrates and no proprietary enzymes. Cost analysis, based on the most expensive reagents required for each assay, puts the MG assay at approximately 50% less expensive than the alternative assays (Table **1**). Cost becomes more of a lead factor as HTS campaigns are increasingly being performed against larger libraries with replicates or multiple concentrations for quantitative HTS (qHTS) [15].

The longer wavelength range for measuring activity also favors the MG assay. A recent trend is to perform qHTS to detect false positives and negatives by analysis of multiple inhibitor concentrations on the assay [15]. However, this increases enormously the number of assays needed to be performed. An alternative method focuses on a reporting wavelength that is minimally impacted by library interference caused by absorbance or autofluorescence of a compound. Data collected by NIH Chemical Genomics Center (NCGC), a member of the NIH Molecular Libraries Screening Centers Network (MLSCN), illustrated that from a typical compound library of 58,450 compounds, 6,462 compounds exhibited emission and excitation wavelengths at 340 nm and a 450 nm (PubChem AID: 590). No compounds were detected when the same library was screened using excitation and emission wavelengths of 570 nm and 647 nm (PubChem AID: 592). Since absorbance of light is a requirement for excitation, MG, with its wavelength range between 590 and 650 nm, would be expected to have minimal interference from current compound libraries used for HTS [16].

A recent study suggests that the MG assay could have the potential to be adapted to a 384-well assay format [17]. In another study, it was shown that a standalone, multi-dispensing system could be used to semi-automate a phosphatase assay for HTS and demonstrated feasibility against a small library of 3,280 compounds [18]. Although this partially-automated method was successful, it still required substantial human intervention to track reaction times and to transfer plates between devices. As with cost, these human tasks can become daunting as substantially

larger libraries and replication become prevalent in modern HTS and qHTS campaigns. Finally, another major concern of the MG assay has been raised regarding the use of concentrated sulfuric acid during the development step since hydrolysis of ATP could occur over time thereby degrading the quality of the results for HTS studies [19].

To address the issues and concerns described above, we have developed a fully automated version of the assay MG assay in a 384-well format capable of screening over 10,000 compounds, in duplicate in a 10-h work day using a relatively simple liquid-handling robot. Moreover, we have applied this assay to the pyrophophatases OSB-CoA synthetase and NMAT, screening 100,080 compounds against each target in an automated HTS format. Finally, we explore the practical nature of implementing the MG assay on small-scale HTS platforms as well as data quality and throughput.

MATERIALS AND METHODS

Sources of Materials

Dimethyl sulfoxide (DMSO), bovine serum albumen (BSA), nicotinate adenine mononucleotide (NaMN), inorganic pyrophosphatase (IPP) from *S. cerevisiae,* malachite green, nicotinate adenine dinucleotide (NaAD), ATP, sodium phosphate, ammonium molybdate, magnesium, Tween 20, sulfuric acid and CoA were all purchased from Sigma-Aldrich. O-Succinylbenzoate (OSB) was synthesized according to previously described methods [20]. Transparent, 384-well plates (Matrix ScreenMates) were used for all HTS and assay optimization. All compound libraries were sourced from Chembridge. His-tagged NMAT and OSB-CoA synthetase proteins were prepared using established protocols [4, 6].

Malachite Green Dye Preparation

The malachite green dye mixture was prepared in 2 L batches in accordance with previously described methods [21]. In short, 300 mL of 36 N sulfuric acid stock was mixed with 1.5 L of water and then cooled down to room temperature. Malachite green powder (2.2 g) was then added and mixed by stirring with a magnetic stir bar and stir plate. Prior to use, 10 mL of the malachite green dye was mixed with 2.5 mL of 7.5% ammonium molybdate and 0.2 mL 11% (v/v) Tween 20. The final mixture, defined as the malachite green development solution was added in a 1:4 ratio to reactions and incubated for 15 min prior to being read at either 623 nm or 612 nm.

Absorbance Spectra and Pi Standard Curves

Absorbance spectra and P_i standard curves were generated by addition of various amounts of P_i to 200 μL of either NMAT HTS reaction conditions (30 mM Tris pH 7.5 250 mM NaCl, 1 mM $MgCl_2$, 15 μM NaMN, and 124.9 μM ATP) or OSB-CoA synthetase HTS reaction conditions (50 mM Tris HCl 7.5, 1 mM $MgCl_2$, 8 μM OSB, 16 μM ATP, 128 μM CoA and 100 mM NaCl). Absorbance spectra were measured using a Varian Cary 50 Bio variable-wavelength spectrometer using 1 mL cuvettes with 1.0 cm pathlengths. In contrast, standard P_i measurements were performed using a Molecular Devices SpectraMax 384 variable wavelength spectrometer using transparent Falcon 96-well assay plates.

384 Format Assay Miniaturization and Optimization for NMAT and OSB-CoA Synthetase HTS

Experiments to optimize release of PP_i for OSB-CoA synthetase and NMAT reactions were conducted in 384-well plates by varying enzyme concentrations and reaction incubation time. For OSB-CoA synthetase reactions, a mixture of 8 μM OSB, 16 μM ATP, 128 μM CoA, and 1 mM $MgCl_2$ was used to assay activity over a 15 min interval. Similar NMAT reactions were conducted using a mixture of 15 μM NaMN, 124.9 μM ATP, and1 mM $MgCl_2$ over a 14.5 min interval. Both enzyme reactions were quenched by the addition of the malachite green development solution. The effect of 2.5% DMSO and 1.5 μM BSA on enzyme activity were also determined with assays measured using the Molecular Devices SpectraMax 384 variable wavelength spectrometer. All reactions were carried out at 23 ^oC and included 0.15 U/mL of the coupling enzyme, IPP.

The product of the reaction, NaAD, was used as a control inhibitor at a single concentration of 28.6 μM for the purpose of assay validation. A concentration range of 15 to 1000 μM of NaAD was used to determine the IC_{50} values for both the MG and MESG assays. The conditions used for the IC_{50} value determination of NaAD for the MG assay were otherwise unchanged from HTS assay conditions. For the MESG assay, the conditions were the same as MG conditions except that 0.5 U of PNP and 300 μM of MESG were added. The activity of NMAT in the MESG assay was monitored continuously over time at an absorbance wavelength of 360 nm as previously described [4, 6]. All IC_{50} curves were fit to the equation $\%I = 100\% / (1 + (Ki/[NaAD]))$ using non-linear regression and the Enzyme Kinetics Module in the program SigmaPlot (Systat)... The percent inhibition values (%I) were calculated using [(sample)-(negative control)]/[([positive control]-[negative control] X 100%.

Compound Library Source and Composition

Compounds were sourced from a two libraries acquired from ChemBridge. Library 1 (Diver Set/CNS Set) contained 50,080 compounds, and Library 2 (Novacore) contained 50,000 compounds. Compounds in both libraries obey Lipinski rules but differ in their diversity [22]. Compounds in Library 1 were selected to maximize diversity, whereas compounds in Library 2 were centered on derivatives of 47 different precursor templates. The 384-well daughter plates used in the study were comprised of 320 compounds from four 96 well mother plates that contained 80 compounds each at 10 mM in DMSO, resulting in 157 daughter plates. The final daughter plate layout contained 16 positive control wells and 16 negative control wells

Automated Screening Procedure

Fully automated, high throughput screens of 100K compounds against OSB-CoA synthetase and NMAT were performed in duplicate using a Tecan Freedom Evo 200 liquid handling station. The robotics platform is equipped with a mounted 3X3 Temo 96 tip pipetting head, fixed-tip,

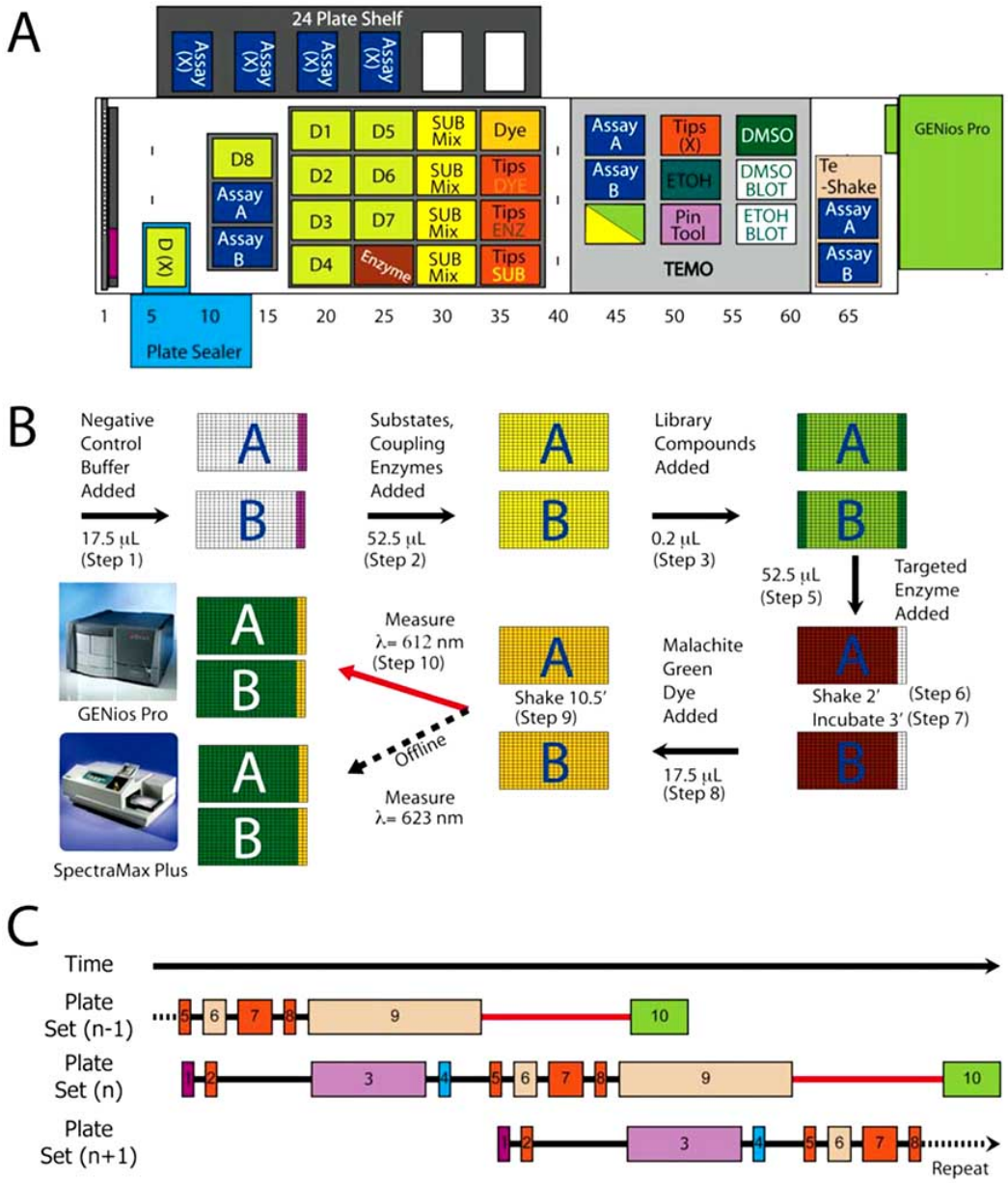

Fig. (2). Schematics for the Robotics Deck Layout, Assay Flow and Plate-Set Scheduling. (**A**) TECAN Freedom Evo deck layout of reagents and robotic components for OSB-CoA synthetase and NMAT. Boxes represent locations of substrates (yellow), library daughter plates (olive), NMAT/OSB-CoA synthetase (brown), DMSO (green), ethanol (teal), blotting paper (white), 384-pin tool (lavender), tips (dark orange), negative control buffer (magenta), and assay plates (blue). Deck locations that are visited multiple types of reagent are colored proportionately according those reagents where as locations visited by different plates of the same type are annotated with (X). (**B**) Assay flow chart. Plate sets are shown as their respective replicates (**A**, **B**) with wells colored to corresponded to well location and reagent added. (**C**) Boxes are shaded according to platform components being utilized. Orange boxes indicate a Temo 3X3 in a 96 head-dispense mode and lavender boxes represent the Temo 3X3 when fitted with a 384-pin tool. Tan boxes represents a TeShake, blue boxes an Abgene 300 plate sealer, and magenta boxes the LiHa arm. The red line and green shaded box represents a GeniosPro plate reader measuring absorbance values at 612 nm during the NMAT enzyme HTS runs. All boxes are scaled according to time, with the largest box equating to 10.5 min. Numbers correspond to; (1) the addition of a negative control, (2) substrate addition, (3) compound addition, (4) library daughter plate sealing, (5) enzyme addition, (6) 2 min shake, (7) 3 min reaction incubation, (8) malachite green development solution addition, and (9) a 10.5 min shake for development. In-line assay detection (10) and red lines denote items that pertain only to the NMAT HTS screen.

liquid-handling arm (Liha Arm), plate transfer robot, automated plate sealer (Abgene ALPS-300), and a Tecan orbital shaker (Te-shake) (Fig. **2A**). All compounds were assayed in duplicate by simultaneously processing two separate assay plates (Fig. **2B**). To achieve simultaneous operation of all of the main robotic elements, the Temo, Te-shake, and Liha operations were synchronized in a manner to allow for up to three plate sets to be processed in different phases of the assay at the same time. The precise timing scheme for each step illustrated in Fig (**2B**) is presented in Fig. (**2C**).

Overall, OSB-CoA synthetase and NMAT HTS assays followed the same nine step process which required only three major liquid addition steps to each well (Fig. **2B**). Step 1 involved adding 17.5 µL of each enzyme's respective enzymatic buffer solution, containing no enzyme, to the 16 negative control wells per plate. Step 2, a 52.5 µL mixture of desired substrates was then added. Subsequently, during step 3, 0.2 µL of 10 mM compound stocks in DMSO were dispensed *via* two passes of a V&P Scientific 100 nL 384-pin tool. Daughter plates were sealed immediately after use by an ALP-300 (Abgene) plate sealer during step 4.

To initiate enzymatic reactions in step 5, 17.5 µL of solution containing either 100 nM OSB-CoA synthetase or 50 nM NMAT was added for a final concentration of 25 nM and 12.5 nM. Plates were shaken at 1600 rpm for 2 min (step 6) and allowed to incubate at 23 °C for an additional 3 min (step 7) prior to being quenched by 17.5 µL malachite green development solution (step 8). In step 9, each plate set was then shaken at 1600 rpm for 10.5 min to allow for development.

For detection of enzyme activity in step 10, we decided to evaluate the logistical and timing benefits of using a deck-accessible plate reader versus one located in separate location of the lab, i.e. not attached to the robot deck, since it is anticipated that different labs will have one or the other setup. We therefore conducted the NMAT screen using the deck-accessible plate reader and the OSB-CoA synthetase assays with the offline detector. The absorbance values for the NMAT plate sets were read immediately after development by a robot accessible GENios Pro monochromatic filter spectrometer at 612 nm (step 10). In contrast, plates for the OSB-CoA synthetase assay were stored on the deck for up to the length of 6 plate sets (2.25 h) prior to being transported manually to a Molecular Devices SpectraMax 384 variable wavelength spectrometer and read at 623 nm. Final concentrations for the OSB-CoA synthetase HTS were 28.5 µM compound, 7.75 µM OSB, 15.5 µM ATP, 124 µM CoA, 50 mM Tris HCl 7.5, 1 mM $MgCl_2$, 100 mM NaCl, 1.5 µM BSA, and 0.15 U/mL IPP. For NMAT HTS, final concentrations were 28.5 µM compound, 15µM NaMN, 124.9 µM ATP, and 1 mM $MgCl_2$.

Data from all screens were processed using a custom program script based on Perl language that was developed by the authors. This program provided matching of sample wells to compound ID numbers and raw absorption data as well as calculation of percent inhibition of each sample well and its replicate. Mean inhibition and duplicate plate set Z'-factor (Z_{DPS}) values were also provided by the program using Eq. (1)-(2).

$$\% \text{ Inhibition} = \frac{\left(\text{Abs}_{\text{sample}} - \text{Abs}_{\mu -}\right)}{\left(\text{Abs}_{\mu +} - \text{Abs}_{\mu -}\right)} \qquad \text{Eq. (1)}$$

$$Z_{DPS} = 1 - \frac{\left(3\sigma_{c+} + 3\sigma_{c-}\right)}{|\mu_{c+} + \mu_{c-}|} \qquad \text{Eq. (2)}$$

Both the Z_{DPS}-factor and mean inhibition calculations used standard deviations (σ) and means (µ) that were based on the 32 control wells, either positive or negative, sourced from both replicate plates.

RESULTS AND DISCUSSION

Optimization of Malachite Green Reagent for OSB-CoA Synthetase and NMAT Reaction Conditions

Traditional advantages for using a colorimetric assay such as MG are its ease of measurement, simplicity of instrumentation, and potentially high signal-to-noise ratio. Added to these, the MG assay in particular detects within a wavelength range that minimizes false positives or negatives. The basis for the colorimetric detection of inorganic phosphate *via* MG is tied to the absorbance of the dye-phosphomolybdate complex formed under conditions of low pH during the development stage [16]. The low pH condition also serves as a suitable method for quenching most enzymatic reactions, as most enzymes, including NMAT and OSB-CoA synthetase, are inactive in the 0-3 pH range. However, these conditions also have the tendency to precipitate reaction components, including the enzyme itself [23]. As a result, various detergents and acids have been employed to reduce development time while keeping reaction components soluble [16]. For our studies, we utilized sulfuric acid and Tween 20 as our acid and detergent, a combination based on a previously described immunoassay [21].

In order to determine the optimal wavelength range of signal detection for assays containing components for OSB-CoA synthetase and NMAT reactions, the malachite green reagent was added to solutions containing the respective enzyme reagents, include ATP, at previously determined K_m values, with and without 8 µM inorganic phosphate [4, 6]. An absorbance spectrum of the phosphate containing NMAT and OSB-CoA synthetase samples, after baseline correction against water, produced three peaks at 444 nm, 590 nm, and 630 nm, within the 370 to 800 nm spectral region (Fig. **3A**). For phosphate-free samples, a 444 nm peak was present with almost the same intensity as the phosphate containing samples. Although a peak at 620 nm was also observed, its intensity was minimal in comparison to the phosphate containing spectra in the same range. As a result, we determined the optimum detection range to be between 590 and 630 nm for MG. This range minimized interference from substrates, compound libraries, and protein.

Miniaturization of the Malachite Green Assay for 384-Well Formats

For the purpose of adapting the MG assay for use in 384-well format, a standard curve at 623 nm was generated from multiple concentrations of P_i in wells containing a total reagent volume of 87.5 uL (Fig. **3B**). Robust linear relationships were observed between 0-20 µM P_i for buffers containing reagents for OSB-CoA synthetase and NMAT reactions. Based on the linear relationship observed, we focused on conditions that produced 7.5 µM of pyrophosphate and therefore 15 µM P_i after adding excess inorganic pyrophosphatase. In order to achieve 15 µM P_i generation for OSB-CoA synthetase and NMAT assays, the primary substrates were fixed at 7.75 µM OSB and 15 µM NaMN, respectively. All other reagents involved in the reaction had their concentrations fixed at their respective K_m values to provide for an assay that was sensitive to all forms of inhibition, also known as a balanced assay (Table **2A**, **B**)

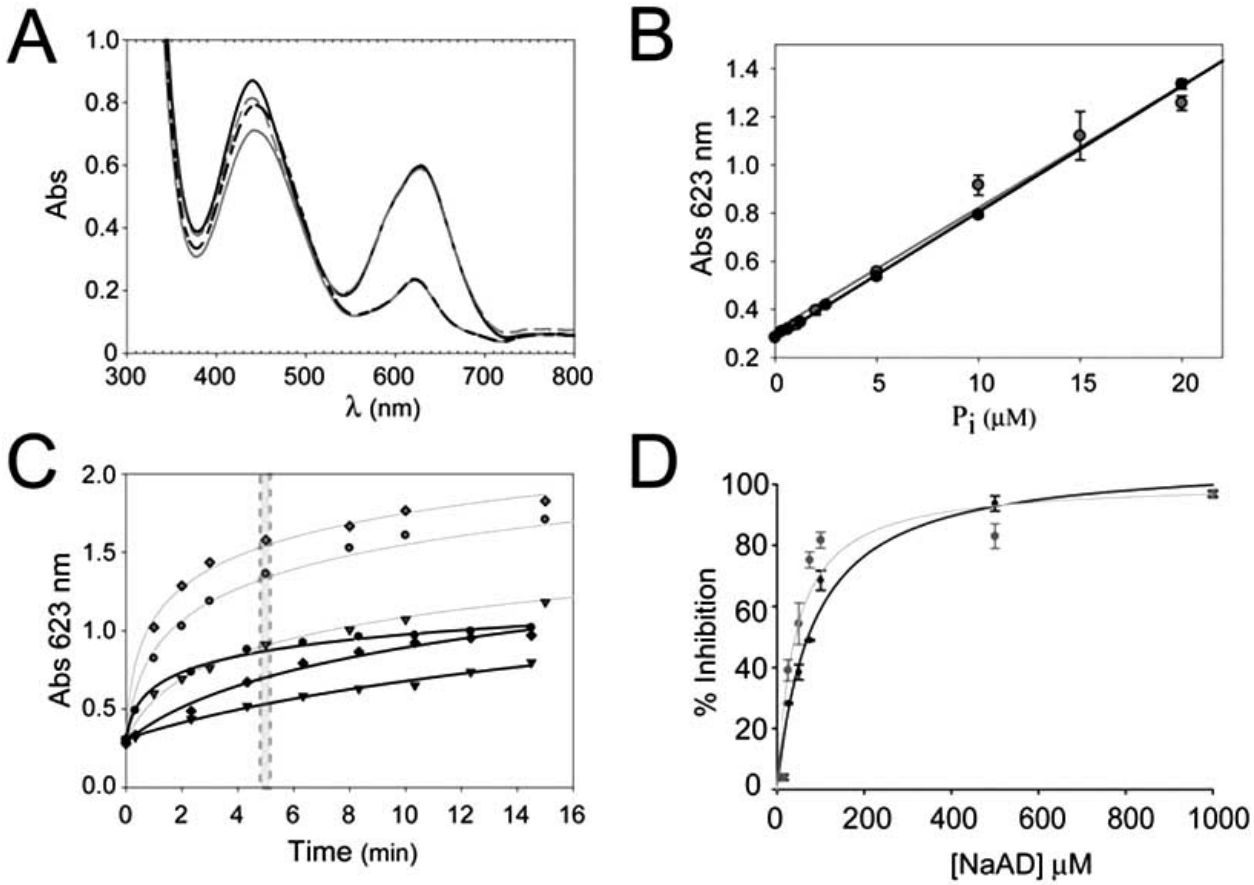

Fig. (3). Malachite green assay optimization for OSB-CoA synthetase and NMAT. (**A**) Spectral scans of OSB-CoA synthetase and NMAT under the conditions of the assay with and without 8 μM P_i. NMAT conditions are indicated with 8 μM P_i (gray; dashed) and without 8 μM P_i (gray; solid). In contrast, OSB-CoA synthetase is depicted as 8 μM P_i (black; solid) and without 8 μM P_i (black; dashed). (**B**) Standard P_i curve for malachite green assay carried out in NMAT reaction conditions (red) and OSB-CoA synthetase reaction conditions (blue). NMAT and OSB-CoA synthetase had slopes of 0.0522 ± 0.0004 (dark red) and 0.0502 ± 0.0018 (blue) respectively. (**C**) Reaction progress curves at varying NMAT concentrations; 12.5 nM (▼), 25 nM (●), and 50 nM (♦) are shown in gray, or at varying OSB-CoA synthetase concentrations; 25 nM (▼), 50 nM (♦), and 100 nM (●) are shown in black. (**D**) The IC_{50} values of NaAD towards NMAT was determined using the MG (black) and the MESG (grey) assays. Data were fit as described in Materials and Methods, and the resulting IC_{50} values were 65.5 ± 5.3 μM for the MG assay and 36.3 ± 4.9 μM for the MESG assay.

[4, 6]. OSB-CoA synthetase and NMAT concentrations were chosen by varying enzyme concentration and monitoring P_i generation over time. OSB-CoA synthetase and NMAT concentrations of 100 nM and 12.5 nM were selected based on the amount of P_i generation over a 5-min time interval (Fig. **3C**). These concentrations proved to be optimal for the automation strategy for reasons described below.

To prevent promiscuous inhibitors from producing false positive hits in the assays and to stabilize OSB-CoA synthetase and NMAT for up to the 3 hrs needed for an automated HTS run, bovine serum albumin (BSA) was added to the assay mixture to a final concentration of 1.5 uM [24]. Since DMSO was expected to be present at concentrations of up to 2.5% as a result of all library compounds being dissolved in 100% DMSO, the effects of both BSA and DMSO on the activities of OSB-CoA synthetase, NMAT, and the coupling enzyme IPP, were tested. No reduction in catalytic activity was observed by the addition of either BSA or DMSO (Table **2C**) [25].

To validate MG's ability to detect potential inhibitors, we chose to capitalize on the inhibition of NMAT by its product NaAD [9]. Validation of an assay normally requires that a proven inhibitor be tested to ensure that a decrease in signal is tied only to the enzyme of interest. In cases where no such inhibitors are known, the product of a reaction can in some incidences serve as an inhibitor. To demonstrate this possibility, we utilized our understanding of the NMAT product inhibition reaction kinetics and used NaAD which is a competitive product inhibitor [6]. We determined the IC_{50} value for NaAD by both the MG endpoint assay and the HTS assay under conditions used in the full HTS screens. The response of NMAT to increasing concentrations of NaAD resulted in an IC_{50} value of 65.5 ± 5.3 μM as determined by the MG assay which is comparable to the IC_{50} of 36.3 ± 4.9 μM determined from continuous MESG assay under the same HTS conditions (Fig. **3D**). Inclusion of 28.6 μM NaAD in sample wells reduced the activity of NMAT by approximately 66% on average. This value falls within the range that would be expected if the concentration of the inhibitor is near its IC_{50} value.

Table 2. OSB-CoA Synthetase and NMAT K_m Substrate Correlations with DMSO and BSA Control Data

A: OSB-CoA Synthetase Substrate Apparent K_m Values[a]				
[ATP]	**4 µM**	**8 µM**	**16 µM**	**32 µM**
OSB K_m (µM)	7.0 ± 0.6	12.8 ± 0.97	8.8 ± 0.7	8.0 ± 0.8
CoA K_m (µM)	68.7 ± 6.5	132 ± 13	149 ± 12	189 ± 19
[OSB]	**2 µM**	**4 µM**	**8 µM**	**16 µM**
ATP K_m (µM)	38.6 ± 6.3	35.9 ± 4.7	19.3 ± 3.8	28.1 ± 3.2
CoA K_m (µM)	94.0 ± 18	126 ± 18	231 ± 18	240 ± 27
[CoA]	**32 µM**	**64 µM**	**128 µM**	**256 µM**
OSB K_m (µM)	0.74 ± 0.19	0.62 ± 0.13	1.4 ± 0.2	1.5 ± 0.2
ATP K_m (µM)	1.4 ± 0.4	2.4 ± 0.4	4.4 ± 0.4	3.2 ± 0.5
B: NMAT Substrate Apparent K_m Values[a]				
[ATP]	**10 µM**	**25 µM**	**300 µM**	**1 mM**
NaMN K_m (µM)	11 ± 1	28 ± 4	15 ± 2	21 ± 1
[NaMN]	**10 µM**	**25 µM**	**300 µM**	**1 mM**
ATP K_m (µM)	119 ± 20	93 ± 15	107 ± 13	142 ± 28
C: DMSO and BSA Effects on Percent Activity[b]				
Enzyme		**2.5% DMSO**	**BSA (1.5 uM)**	**Both**
NMAT		93 ± 3	106 ± 2	99 ± 2
OSB-CoA synthetase		98 ± 3	98 ± 3	97 ± 6
IPP		101 ± 3	102 ± 1	103 ± 1

[a]All K_m determinations were derived from previous kinetic studies of *B. anthracis*' OSB synthetase and NMAT [4, 6]. [b]Percent Activity calculated using the formula, [A_{623} with additives]/ [A_{623} without additives] X 100.

Implementation of an Automated HTS Malachite Green Assay

The implementation of automated high throughput screens on large compound libraries requires that at least two criteria be met, high throughput and reproducibility. To achieve both of these criteria, we chose to develop a robotic scheme that would allow all compounds to be tested in duplicate (Fig. **2**). Our scheme provides for the simultaneous operations of the liquid handling, plate, and 96 multi-dispensing robot arms of a TECAN Freedom Evo 200. As a result, the processing of multiple 384-well assay plates can be performed simultaneously. The final scheme using a robotics platform that can accommodate reagents and consumables for eight plates that can be screened in duplicate during one 2.5 h time period allowed for a throughput of over 10,000 compounds, 24,576 wells total, in a typical ten hour work day.

The throughput was limited in our case only by the lack of on deck storage of reagents and plates. Depending on the assay platform in different labs, we anticipate that the strategy outlined in Fig. (**2**) would be directly scalable pending the liquid handler in use. Although a basic TECAN Freedom Evo 200 was used here, addition of a deck accessible carousel for plate storage and a dedicated reagent dispenser with a large reservoir for this deck, or other similar liquid handlers to include those from CyBio, Beckman Coulter, and Panasonic allows for screening 24,576 compounds in duplicate, 58,982 per 24 h period (Fig. **2A**). In addition to allowing for relatively high throughput capacity, the automation scheme allows for the entire assay to be performed on one robot deck without any manual manipulations or off deck storage of plates, which has been typical of other similar HTS assays [18, 19]. As a result, a substantial increase in reproducibility and time savings were achieved. It would also be possible to run the assays continuously over a 24 h time period assuming that the particular enzyme under study by the investigators is stable over extended time periods. In our case, we found that NMAT and OSB-CoA synthetase were most stable for up to 10 h on the robot deck, and we found it valuable to perform real-time evaluation of Z-factors to ensure the best data quality for our enzymes.

The implementation of the automation scheme also demanded an additional consideration in terms of reaction times and library compound concentrations. To fully utilize the time-saving overlapping method and eliminate dwell time, the reactions were limited to 5 min. This time interval required that the enzyme concentrations be 100 nM for OSB-CoA synthetase and 12.5 nM for NMAT in order to achieve a maximum signal-to-noise ratio (Fig. **3C**). A concentration of 28.5 µM was chosen for the library compounds since this concentration could be readily achieved by two transfers from the 10 mM stock concentrations of the compounds using a 100 nL capacity pin tool within the optimal time frame. This delivery volume also limited the final DMSO concentration to 0.28% which is well below the 2.5% DMSO which is tolerable for both enzymes (Table **2C**).

Beyond the expediency of using 28.5 µM as the final compound concentration in the assay, this concentration was deemed reasonable for the detection of inhibitors with K_i values of below 50 µM. Since the concentrations of the three substrates (OSB, ATP and CoA) used in the assay were within 0.5 to 4 times their K_m values, the detection of inhibitors that could act *via* any mode of inhibition, i.e. noncompetitive, competitive or uncompetitive or mixed, is expected [26]. Since it is unclear at this time as to which mode of inhibition will eventually lead to the best antibiotic against OSB-CoA synthetase, probing for an inhibitor with any mode of action was deemed the best strategy in the initial screening campaign.

Large Scale Screening and Data Processing of a 100K Compound Library

To explore the practicality of using MG for large libraries, OSB-CoA synthetase and NMAT were each screened separately against two libraries comprising approximately 100K commercially available compounds. Positive controls for each of the assays ranged from 0.65 to 1.0 absorbance units at 623 nm for OSB-CoA synthetase, and at 612 nm for NMAT. Negative controls for OSB-CoA synthetase ranged from 0.21 to 0.40 absorbance units, and negative controls for NMAT ranged from 0.17 to 0.19 absorbance units (Fig. **4A**, **B**).

Z'-factors for the assays were calculated using a modified version of the traditional Z'-factor calculation by aggregating all 32 positive controls and 32 negative controls of both

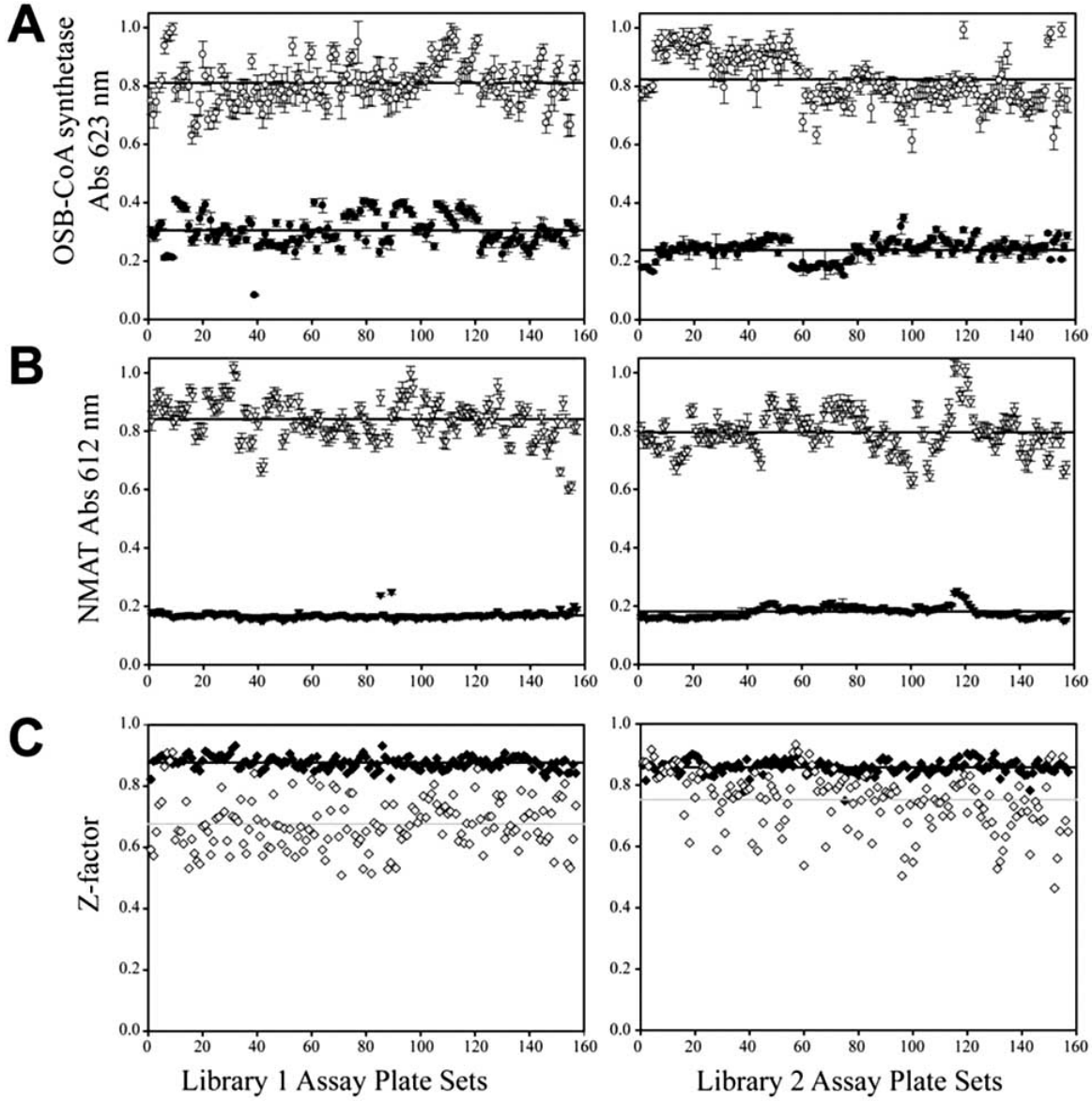

Fig. (4). High throughput screening (HTS) quality factors for OSB-CoA synthetase and NMAT for library 1 and library 2. (**A**) OSB-CoA synthetase positive mean (○) and negative mean (●) calculated using all the control samples from both plate **A** and plate **B** with error bars for standard deviation. Black lines represent the means of positive and negative controls calculated across each library. (**B**) NMAT positive mean (∇) and negative mean (▼) calculated using all the control samples from both plate A and plate B with error bars for standard deviation. Black lines represent the means of positive and negative controls calculated across each library. (**C**) Z_{DPS}-factors calculated from control samples from plate A and plate B of an individual assay plate set. OSB-CoA synthetase Z_{DPS}-factors in (◊) and NMAT (♦). Lines represent the mean Z_{DPS} calculated from each library for the NMAT MG (black) and OSB-CoA synthetase MG (grey) assays.

plates instead of treating each plate independently. This allowed for generation of a "duplicate plate set Z'-factor" (Z_{DPS}). The Z_{DPS}-factor, in comparison to the single plate Z'-factor calculations, does not treat each plate independently but as one plate. As a result, the quality between the replicates is captured in the Z_{DPS}-factor value. All plate sets for NMAT and OSB-synthetase possessed a Z_{DPS}-factor value greater then 0.5, the minimum benchmark for the assays to be considered "excellent assay" [27]. The average Z_{DPS}-factor of the entire screen of 100,080 compounds for the NMAT MG assay was 0.86±0.02 and for the OSB-synthetase MG assay was 0.71±0.09 (Fig **4c**).

The coefficient of variance's (C_v) taken from a typical 384-well plate were consistent or better than previous manual or partially automated HTS applications of MG (Table **3**) [18]. However, the signal-to-noise ratios between the NMAT and OSB-CoA synthetase assays differed significantly. Whereas the NMAT assay had a signal-to-noise ratio of 23.2, the value for OSB-CoA synthetase was only 5.3 when controls were compared from a typical plate. This difference is believed to result partially from OSB-CoA synthetase having a higher absorbance value for the negative control resulting from background absorbance of the reaction components. The OSB-CoA synthetase assay also differed in terms of detection procedures from those of the NMAT

assay which also may have contributed to negative and positive fluctuations in control samples.

Table 3. Typical* Plate Controls

	NMAT Plate A	NMAT Plate B	OSB-CoA Synthetase Plate A	OSB-CoA Synthetase Plate B
Mean Signal**	0.82	0.82	0.81	0.82
Signal C_V	3%	3%	5%	3%
Mean Background**	0.17	0.17	0.35	0.36
Background C_V	1%	1%	3%	2%
Signal/Noise	23.2	23.2	5.3	5.3

*Plate Set 72 from Library 1.
** Absorbance at 623 nm for OSB-CoA synthetase and 612 nm for NMAT.

Although the OSB-CoA synthetase assay was automated up to step 9, we evaluated the logistical and timing issues surrounding off-line detection, a scenario that exists in many labs. The absorbance detection relied on manually transporting the plates to the microplate plate reader and then manually feeding the plates, one-by-one, into the reader. We found such an operation problematic for a number of reasons. First, it was difficult logistically to continue to remove plates from the robot deck and then transport them to the microplate reader though it was in the same room. Second, having to utilize a person full-time to perform this manual operation removes them from more practical exercises such as having them evaluate the quality of the data in real time. Third, due to the impracticality of having each duplicated set of plates measured exactly at the same post-quenching time on our robotics platform, some OSB-CoA synthetase plates were left unmeasured for up to 2.25 h, the length of an OSB-CoA HTS run, before having the absorbance measured at 623 nm. Thus, precise timing of measurements using an offline detector is impractical compared to on-deck detection.

Other issues also arose with offline versus online measurements. As observed with previous assays, the low pH conditions of development can result in the hydrolysis of nucleotides over long time periods, thus affecting both the negative and positive control values [18, 19, 28]. The hydrolysis results not only in a variance in the control absorbance values but also in a variance in Z_{DPS}-factor calculations per each plate set for OSB-CoA synthetase (Fig. **4c**; Table **3**). In comparison, the NMAT assay included detecting absorbance through the use of an on-deck spectrometer that could be accessed by automation (Fig. **2B**, **C**). Thus, each plate set was read in the same time frame of the previous plate set. This time saving technique removed the impact of acid-promoted ATP hydrolysis during the NMAT screen and in return eliminated the fluctuations seen in the OSB-CoA synthetase assay. Moreover, an increase in reproducibility was observed with the NMAT MG assay over the OSB-CoA synthetase assay. By comparing each sample's relationship with its duplicate through a replicate plot, the NMAT sample wells had minimal dispersion from the ideal relationship in comparison to the OSB-CoA synthetase sample wells (Fig. **5A**, **B**). In addition, with the intrinsically lower negative control values, the NMAT assay generated more consistent control and Z_{DPS}-factor values.

Finally, the results from both assays have so far allowed for numerous 'hit' compounds to be identified with IC_{50} values ranging from approximately 1 to 100 μM depending on the percent inhibition cut-off values selected (data not shown). For example, using an automated IC_{50} determination and the MG assay, a typical hit in the OSB-CoA synthetase screen with 33.1 % mean inhibition between the duplicates, resulted in an IC_{50} of 36.7 ± 4.6 (Fig. **5C**). For NMAT, a primary hit with a 56.1 % mean inhibition between the duplicates resulted in an IC_{50} of 20.0 ± 3.3 (Fig. **5D**). Although the primary mode of inhibition (competitive, non-competitive, un-competitive or mixed) for these compounds is currently unknown, these preliminary data indicate that a good range of inhibitory potencies can be detected.

CONCLUSIONS

A large number of current laboratories that perform HTS for drug discovery and molecular probe development do not have the resources necessary for the advanced robotics required for ultra-HTS or qHTS of large libraries. Here we demonstrate a scalable alternative to this approach by screening two ERPs from *B. anthracis* using only a single commercially available liquid handling robot prevalent in the HTS community. Using this assay, small scale robotics platforms such as the one used in these studies can readily screen 20K to 30K wells per 10 to 12 h work day. Importantly, the assay should be scaleable to most robotics systems, including commercial systems such as the kalypsys® screening systems, that are capable of screening up to 500K wells per day.

The subsequent benefits of utilizing this assay strategy are far reaching. As shown, the introduction of even one manual step, such as reading the plates for OSB-CoA synthetase, could introduce unnecessary fluctuations and increase time commitments of the researcher. When the manual step is removed, no detrimental effects on the C_v's, signal-to-noise ratio, or Z'-factors are observed, and the values either exceeded or were comparable to previous studies. Furthermore, automating the reading of assay plates proved to be an effective method of dealing with the issue of ATP hydrolysis at low pH conditions. Not only were no manual steps required while carrying out the assay for NMAT or OSB-CoA synthetase, but once established, no reprogramming was required to adapt the assay between NMAT, OSB-CoA synthetase. Consequently, reprogramming is assumed to be not required to screen other pyrophosphatases or phosphatases in general. In total, this method allowed for a throughput of 10,000 compounds in duplicate per 10 h period, and a total of 100,080 compounds were screened in total for each enzyme. Since many enzymatic pathways, including those that NMAT and OSB-CoA synthetase belong to, normally contain not one but several ERPs, this universal HTS assay could potentially allow for the rapid screening of entire pathways or multiple single enzymatic reactions, at facilities having small-scale liquid handling robotics. In addition, this assay is capable of automating the measurement of IC_{50} values for hit validation and secondary assays, as well as for the determination of kinetic parameters in multi-substrate enzymatic reactions as

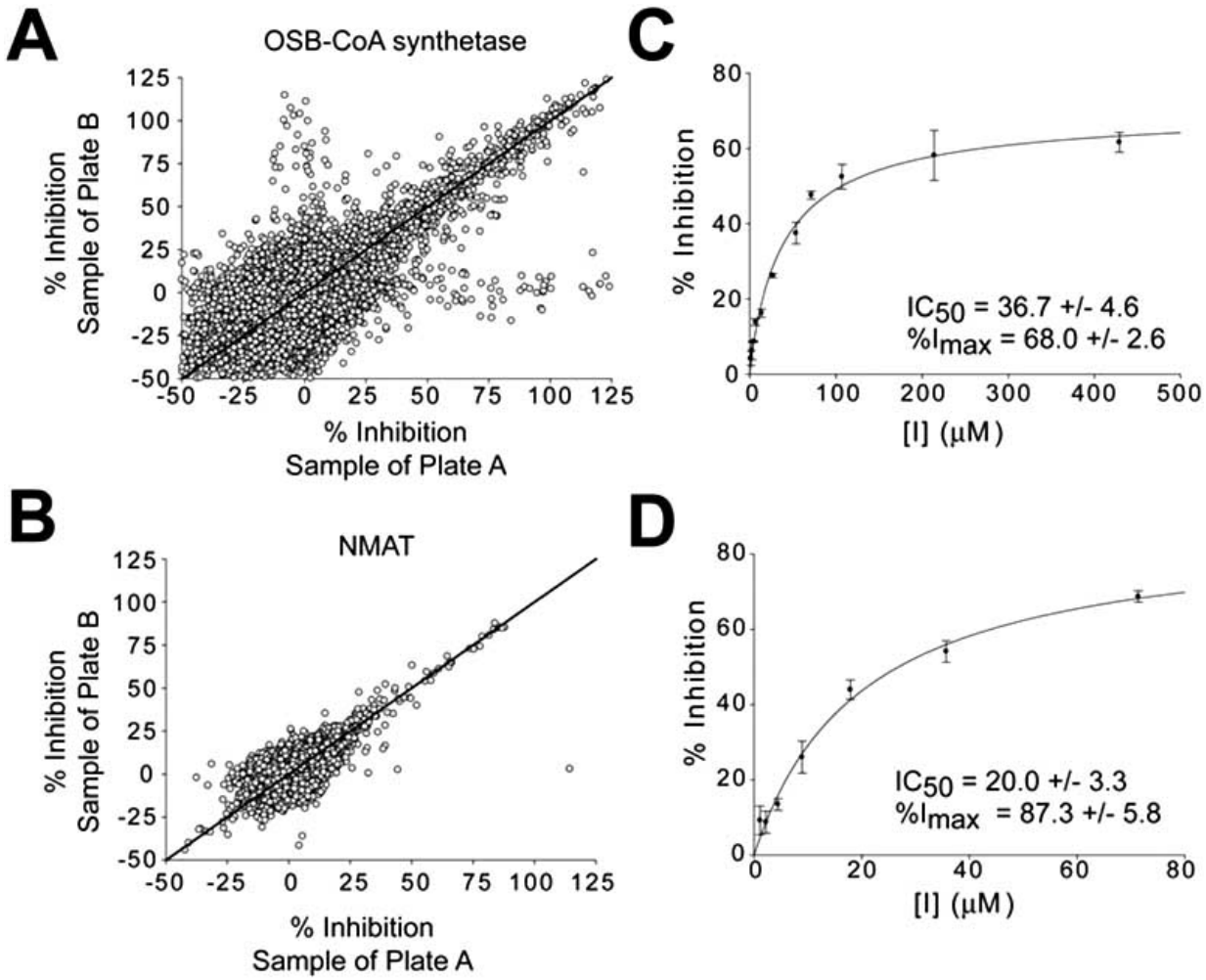

Fig. (5). HTS assay results for OSB-CoA synthetase and NMAT compound library screens. Replicate plots for the percent inhibition resulting from assay sets, i.e. plate **A** versus plate **B**, are shown in (**A**) for the 100,080 compounds screened against OSB-CoA synthetase, and (**B**) for the 100,080 compounds screened against NMAT. The black line in each panel represents an ideal replicate relationship with a slope of 1. Sample wells with large, negative, percent inhibition values, 40 for OSB-CoA synthetase and 12 for NMAT, that can result from machine pippeting errors or compound interference, were omitted to provide greater clarity for comparison of the remaining samples between NMAT and OSB-CoA synthetase. The IC_{50} values for two 'hit' compounds identified from the primary screen were determined for OSB-CoA synthetase (**C**) and NMAT (**D**).

we have demonstrated for NMAT and OSB-CoA synthetase [4, 6]. The HTS assay for ERPs described here should therefore provide the research community with a scalable efficient screening assay for multiple robotics platforms as well as provide an opportunity for assay design to move beyond an enzyme target based HTS to one that is pathway or organism oriented.

ACKNOWLEDGEMENTS

This work was funded by a grant from NIH/NIAID (U19 AI056575). We would like to thank Dick Mitchell, Systat for use of a beta version of SigmaPlot HTS macro, Institute for Tuberculosis Research for use of their chemical library, and Dr. David Crich's lab at University of Illinois Chicago for synthesizing the OSB used in the study.

REFERENCES

[1] Kobayashi, K.; Ehrlich, S.D.; Albertini, A.; Amati, G.; Andersen, K.K.; Arnaud, M.; Asai, K.; Ashikaga, S.; Aymerich, S.; Bessieres, P.; Boland, F.; Brignell, S.C.; Bron, S.; Bunai, K.; Chapuis, J.; Christiansen, L.C.; Danchin, A.; Débarbouille, M.; Dervyn, E.; Deuerling, E.; Devine, K.; Devine, S.K.; Dreesen, O.; Errington, J.; Fillinger, S.; Foster, S.J.; Fujita, Y.; Galizzi, A.; Gardan, R.; Eschevins, C.; Fukushima, T.; Haga, K.; Harwood, C.R.; Hecker, M.; Hosoya, D.; Hullo, M.F.; Kakeshita, H.; Karamata, D.; Kasahara, Y.; Kawamura, F.; Koga, K.; Koski, P.; Kuwana, R.; Imamura, D.; Ishimaru, M.; Ishikawa, S.; Ishio, I.; Le Coq, D.; Masson, A.; Mauël, C.; Meima, R.; Mellado, R.P.; Moir, A.; Moriya, S.; Nagakawa, E.; Nanamiya, H.; Nakai, S.; Nygaard, P.; Ogura, M.; Ohanan, T.; O'Reilly, M.; O'Rourke, M.; Pragai, Z.; Pooley, H.M.; Rapoport, G.; Rawlins, J.P.; Rivas, L.A.; Rivolta, C.; Sadaie, A.; Sadaie, Y.; Sarvas, M.; Sato, T.; Saxild, H.H.; Scanlan, E.; Schumann, W.; Seegers, J.F.; Sekiguchi, J.; Sekowska, A.; Séror, S.J.; Simon, M.; Stragier, P.; Studer, R.; Takamatsu, H.; Tanaka, T.; Takeuchi, M.; Thomaides, H.B.; Vagner, V.; van Dijl, J.M.; Watabe, K.; Wipat, A.; Yamamoto, H.; Yamamoto, M.; Yamamoto, Y.; Yamane, K.; Yata, K.; Yoshida, K.; Yoshikawa, H.; Zuber, U.; Ogasawara, N. Ogasawara, essential *Bacillus subtilis* genes. *Proc. Natl. Acad. Sci. USA*, **2003**, *100*(8), 4678-4683.

[2] Bryant, R.W.; Bentley, R. Menaquinone biosynthesis: conversion of o-succinylbenzoic acid to 1, 4-dihydroxy-2-naphthoic acid and menaquinones by *Escherichia coli* extracts. *Biochemistry*, **1976**, *15*(22), 4791-4796.

[3] Kwon, O., Bhattacharyya, D.K.; Meganathan, R. Menaquinone (vitamin K-2) biosynthesis: overexpression, purification, and properties of o-succinylbenzoyl-coenzyme a synthetase from *Escherichia coli*. *J. Bacteriol*., **1996**, *178*(23), 6778-6781.

[4] Tian, Y.; Mesecar, A.D. Bacillus anthracis o-Succinylbenzoyl-CoA synthetase: reaction kinetics and a novel inhibitor mimicking its reaction intermediate. *Biochemistry*, **2008**, *47*, 12434-12447.

[5] Bergman, N.H.; Anderson, E.C.; Swenson, E.E.; Janes, B.K.; Fisher, N.; Niemeyer, M.M.; Miyoshi, A.D.; Hanna, P.C. Transcriptional profiling of Bacillus anthracis during infection of host macrophages. *Infect. Immun.*, **2007**, *75*(7), 3434-3444.

[6] Sershon, S.C.; Santarsiero, B.D.; Mesecar, A.D. Kinetic and structural evidence of negative cooperativity in substrate binding to nicotinate mononucleotide adenylyltransferase (NMAT) from *Bacillus anthracis*. *J. Mol. Biol.*, **2008**, *385*, 867-888.

[7] Bhattacharyya, D.K.; Kwon, O.; Meganathan, R. Vitamin K2 (menaquinone) biosynthesis in *Escherichia coli*: evidence for the presence of an essential histidine residue in o-succinylbenzoyl coenzyme A synthetase. *J. Bacteriol.*, **1997**, *179*(19), 6061-6065.

[8] Zheng, R.; Blanchard, J.S. Steady-state and pre-steady-state kinetic analysis of Mycobacterium tuberculosis pantothenate synthetase. *Biochemistry*, **2001**, *40*(43), 12904-12912.

[9] Sershon, S.C.; Santarsiero, B.D.; Mesecar, A.D. Kinetic and structural evidence of negative cooperativity in substrate binding to nicotinate mononucleotide adenylyltransferase (NMAT) from *Bacillus anthracis*. *J. Mol. Biol.*, **2009**, *385*(3), 867-888.

[10] Ahmadian, A.; Ehn, M.; Hober, S. Pyrosequencing: history, biochemistry and future. *Clin. Chim. Acta.*, **2006**, *363*(1-2), 83-94.

[11] Nyren, P.; Lundin, A. Enzymatic method for continuous monitoring of inorganic pyrophosphate synthesis. *Anal. Biochem*., **1985**, *151*(2), 504-509.

[12] Pais, J.E.; Bowers, K.E.; Stoddard, A.K.; Fierke, C.A. A continuous fluorescent assay for protein prenyltransferases measuring diphosphate release. *Anal. Biochem*., **2005**, *345*(2), 302-311.

[13] Webb, M.R. A continuous spectrophotometric assay for inorganic phosphate and for measuring phosphate release kinetics in biological systems. *Proc. Natl. Acad. Sci. USA*, **1992**, *89*(11), 4884-4887.

[14] Itaya, K.; Ui, M. A new micromethod for the colorimetric determination of inorganic phosphate. *Clin. Chim. Acta*., **1966**, *14*(3), 361-366.

[15] Inglese, J., Auld, D.S.; Jadhav, A.; Johnson, R.L.; Simeonov, A.; Yasgar, A.; Zheng, W.; Austin, C.P. Quantitative high throughput screening: a titration-based approach that efficiently identifies biological activities in large chemical libraries. *Proc. Natl. Acad. Sci. USA*, **2006**, *103*(31), 11473-11478.

[16] Van Veldhoven, P.P.; Mannaerts, G.P. Inorganic and organic phosphate measurements in the nanomolar range. *Anal. Biochem*., **1987**, *161*(1), 45-48.

[17] Bernal, C., Palacin, C.; Boronat, A.; Imperial, S. A colorimetric assay for the determination of 4-diphosphocytidyl-2-C-methyl-D-erythritol 4-phosphate synthase activity. *Anal. Biochem.,* **2005**, *337*(1), 55-61.

[18] Rowlands, M.G., Newbatt, Y.M.; Prodromou, C.; Pearl, L.H.; Workman, P. Aherne, W. High throughput screening assay for inhibitors of heat-shock protein 90 ATPase activity. *Anal. Biochem.*, **2004**, *327*(2), 176-183.

[19] Mok, M.T.S.; Edwards, M.R. Critical sources of error in colorimetric assay for UDP-N-acetylglucosamine pyrophosphorylase. *Anal. Biochem*., **2005**, *343*(2), 341-343.

[20] Leete, E.; Bodem, G.B. Biosynthesis of shihunine in Dendrobium pierardii. *J. Am. Chem. Soc.*, **1976**, *98*(20), 6321-6325.

[21] Baykov, A.A.; Evtushenko, O.A.; Avaeva, S.M. A malachite green procedure for orthophosphate determination and its use in alkaline phosphatase-based enzyme immunoassay. *Anal. Biochem.,* **1988**, *171*(2), 266-270.

[22] Lipinski, C.A., Lombardo, F.; Dominy, B.W.; Feeney, P.J. Experimental and computational approaches to estimate solubility and permeability in drug discovery and development settings. *Adv. Drug Deliv. Rev.*, **2001**, *46*(1-3), 3-26.

[23] Geladopoulos, T.P.; Sotiroudis, T.G.; Evangelopoulos, A.E. A malachite green colorimetric assay for protein phosphatase activity. *Anal. Biochem*., **1991**, *192*(1), 112-116.

[24] McGovern, S.L.; Caselli, E.; Grigorieff, N.; Shoichet, B.K. A common mechanism underlying promiscuous inhibitors from virtual and high throughput screening. *J. Med. Chem.,* **2002**, *45*(8), 1712-1722.

[25] Garzon, J.; DeFelipe, J.; Rodriguez, J.R.; DeAntonio, I.; Garcia-Espana, A.; Sanchez-Blazquez, P. Transport of CSF antibodies to Galpha subunits across neural membranes requires binding to the target protein and protein kinase C activity. *Brain Res. Mol. Brain Res.*, **1999**, *65*(2), 151-166.

[26] Copeland, R.A. Mechanistic considerations in high throughput screening. *Anal. Biochem.*, **2003**, *320*(1), 1-12.

[27] Zhang, J.H.; Chung, T.D.; Oldenburg, K.R. A simple statistical parameter for use in evaluation and validation of high throughput screening assays. *J. Biomol. Screen.*, **1999**, *4*(2), 67-73.

[28] Quan, A.; Robinson, P.J. Rapid purification of native dynamin I and colorimetric GTPase assay. *Methods Enzymol.,* **2005**, *404*, 556-569.

Received: October 22, 2008 **Revised: January 21, 2009** **Accepted: March 27, 2009**